

# Experimental Observation of Environment-induced Sudden Death of Entanglement

M. P. Almeida, F. de Melo, M. Hor-Meyll, A. Salles, S. P. Walborn,\* P. H. Souto Ribeiro, and L. Davidovich

*Instituto de Física, Universidade Federal do Rio de Janeiro,  
Caixa Postal 68528, Rio de Janeiro, RJ 21941-972, Brazil*

(Dated: July 16, 2018)

We demonstrate the difference between local, single-particle dynamics and global dynamics of entangled quantum systems coupled to independent environments. Using an all-optical experimental setup, we show that, while the environment-induced decay of each system is asymptotic, quantum entanglement may suddenly disappear. This “sudden death” constitutes yet another distinct and counter-intuitive trait of entanglement.

The real-world success of quantum computation [1, 2, 3] and communication [4, 5, 6, 7, 8, 9, 10] relies on the longevity of entanglement in multi-particle quantum states. In this respect, the presence of decoherence [11] in communication channels and computing devices, which stems from the unavoidable interaction between these systems and the environment, presents a considerable obstacle, as it degrades the entanglement when the particles propagate or the computation evolves. Decoherence leads to both local dynamics, associated with single-particle dissipation, diffusion, and decay, and to global dynamics, which may provoke the eventual disappearance of entanglement [12, 13, 14, 15, 16]. This phenomenon, known as “entanglement sudden death” [16], is strikingly different from the single-particle dynamics, which occur asymptotically, and as a result has been the focus of much recent theoretical work [12, 13, 14, 15, 16]. We have experimentally demonstrated the sudden death of entanglement of a two-qubit system under the influence of independent environments. Our all-optical setup allows for the controlled investigation of a variety of dynamical maps that describe fundamental processes in quantum mechanics and quantum information.

Consider a two-level quantum system  $S$  (upper and lower states  $|e\rangle$  and  $|g\rangle$ , respectively) under the action of a zero-temperature reservoir  $R$ . At zero temperature, the reservoir  $R$  is in the  $|0\rangle_R$  (vacuum) state, and the  $S - R$  interaction can be represented by a quantum map, known as the amplitude decay channel [1, 2]:

$$\begin{aligned} |g\rangle_S \otimes |0\rangle_R &\rightarrow |g\rangle_S \otimes |0\rangle_R \\ |e\rangle_S \otimes |0\rangle_R &\rightarrow \sqrt{1-p} |e\rangle_S \otimes |0\rangle_R + \sqrt{p} |g\rangle_S \otimes |1\rangle_R. \end{aligned} \quad (1)$$

Under this map, the lower state  $|g\rangle$  is not affected, while the upper state  $|e\rangle$  either decays to  $|g\rangle$  with probability  $p$ , creating one excitation in the environment (state  $|1\rangle_R$ ), or remains in  $|e\rangle$ , with probability  $1 - p$ . This would be the situation, for instance, in the spontaneous emission of a two-level atom. In this case, the state  $|1\rangle_R$  would correspond to one photon in the reservoir. Under the Markovian approximation,  $p = 1 - \exp(-\Gamma t)$ , that is, the decay probability approaches unity exponentially in time. As an initial pure state  $a|e\rangle + b|g\rangle$  decays, it gets entangled with the environment, gradually losing its coherence and its purity over time. Complete decay only occurs asymptotically in time ( $p \rightarrow 1$  when  $t \rightarrow \infty$ ), when the two-level system is again described by the pure state

$|g\rangle$ .

Now consider two entangled qubits that decay according to the map (1). How does the entanglement of the two-qubit system evolve? Does it mimic the asymptotic decay of each qubit, disappearing at  $t \rightarrow \infty$ , or does it disappear at some finite time? This question has been explored theoretically [12, 13, 14, 15, 16], but up to now there has been no experimental investigation of the relation between the global entanglement dynamics and the local decay of the constituent subsystems.

In order to adequately answer these questions, one needs a formal definition of entanglement. A convenient measure of entanglement for a two-qubit system is the *concurrence*  $C$ , introduced by Wootters [17], and given by

$$C = \max\{0, \Lambda\}, \quad (2)$$

where

$$\Lambda = \sqrt{\lambda_1} - \sqrt{\lambda_2} - \sqrt{\lambda_3} - \sqrt{\lambda_4}, \quad (3)$$

and the quantities  $\lambda_i$  are the positive eigenvalues, in decreasing order, of the matrix

$$\rho(\sigma_y \otimes \sigma_y) \rho^* (\sigma_y \otimes \sigma_y), \quad (4)$$

where  $\rho$  is the density matrix of the bipartite system. Here  $\sigma_y$  is the second Pauli matrix and the conjugation occurs in the computational basis  $\{|00\rangle, |01\rangle, |10\rangle, |11\rangle\}$ .  $C$  quantifies the amount of quantum correlation that is present in the system, and can assume values between 0 (only classical correlations) and 1 (maximal entanglement).

For the dynamics given by Eq. (1), and an initial state of the form  $|\Phi\rangle = |\alpha| |gg\rangle + |\beta| \exp(i\delta) |ee\rangle$ , the entanglement decay dynamics depends on the relation between  $|\alpha|$  and  $|\beta|$  [15]. Concurrence in this case is given by

$$C = \max\{0, 2(1-p)|\beta|(|\alpha| - p|\beta|)\}. \quad (5)$$

From this expression, one can see that for  $|\beta| < |\alpha|$ , entanglement disappears only when the individual qubits have completely decayed ( $p = 1$ ), while for  $|\beta| > |\alpha|$ , entanglement disappears for  $p = |\alpha/\beta| < 1$ , which corresponds to a finite time. This phenomenon has been called “entanglement sudden death” [16]. Since the concurrence of the initial state ( $p = 0$ ) is  $C = 2|\alpha\beta|$ , the entanglement dynamics of two states with the same initial concurrence can be quite different.

Photons are a very useful experimental tool for demonstrating these properties and, more generally, for studying quantum channels like the one given in Eq. (1), since the decoherence mechanisms can be implemented in a controlled manner. Let us associate the  $H$  and  $V$  polarizations of a photon respectively to the ground and excited states of the two-level system  $S$ . The reservoir  $R$  in turn is represented by two different momentum modes of the photon. Fig. 1a shows a Sagnac-like interferometer which implements the amplitude-decay channel (1) for a single qubit. A photon, initially in the incoming part of mode  $a$ , is split into its horizontal ( $H$ ) and vertical ( $V$ ) polarization components by a polarizing beam splitter (PBS1). Let us ignore the half-wave plates HWP1 and HWPC momentarily. The  $V$ -polarization component is reflected and propagates through the interferometer in the clockwise direction, and, if unaltered, reflects through PBS1 into

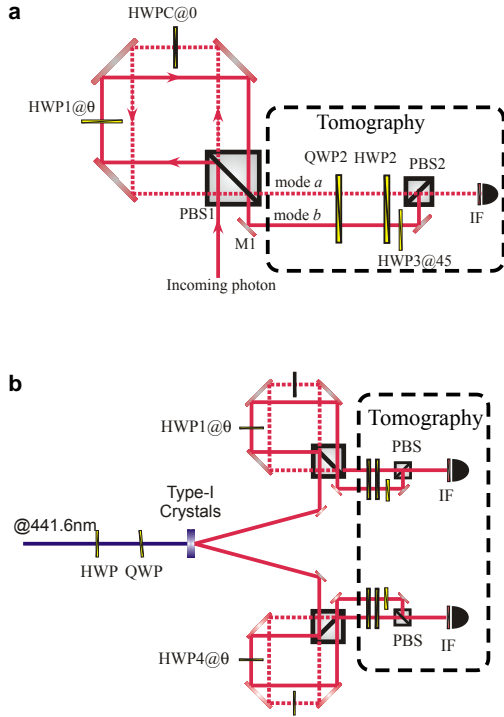


FIG. 1: Experimental setup. **a** Amplitude decay channel for a single photonic qubit. Due to the polarized beam splitter PBS1, the  $H$  and  $V$  components of polarized photons propagate respectively along counter-clockwise and clockwise paths within the interferometer. With half-wave plate HWP1 set at  $0^\circ$ , they are coherently recombined into the outgoing spatial mode  $a$ , which represents the “vacuum state” of the reservoir. For other angles of HWP1, the  $V$ -component undergoes a rotation, corresponding to its probabilistic “decay” into the  $H$ -component, which PBS1 sends to outgoing mode  $b$ , representing the “one-excitation state” of the reservoir. Wave plates HWP2 and QWP2, together with PBS2, are used for tomography of the polarization state of outgoing modes  $a$  and  $b$ , which are recombined incoherently on PBS2 using HWP3, and sent to the same detector. IF is an interference filter. **b** Amplitude decay channel applied to entangled qubits. The entangled state is generated by parametric down-conversion in type-I non-linear crystals.

the outgoing part of mode  $a$ . The  $H$ -polarization component is transmitted and propagates through the interferometer in the counter-clockwise direction and transmits through PBS1, also into the outgoing part of mode  $a$ . However, the interferometer is aligned so that the two paths are spatially separated, making it possible to manipulate the  $H$  and  $V$  polarization components independently.

To realize the amplitude decay given in map (1), we use HWP1 to rotate the polarization of the  $V$  component to  $\cos(2\theta)|V\rangle + \sin(2\theta)|H\rangle$ , where  $\theta$  is the angle of HWP1. Suppose that an incoming photon is  $V$ -polarized. When this photon exits the interferometer through PBS1, it is transmitted into mode  $b$  with probability  $p = \sin^2(2\theta)$  and reflected into mode  $a$  with probability  $\cos^2(2\theta)$ . This evolution can thus be described by  $|V\rangle|a\rangle \rightarrow \sqrt{1-p}|V\rangle|a\rangle + \sqrt{p}|H\rangle|b\rangle$ . Identifying the outgoing modes  $a$  and  $b$  (which correspond to orthogonal spatial modes) as the states of the reservoir with zero and one excitation, respectively, this operation is equivalent to that on the  $|e\rangle|0\rangle_R$  state in map (1). An incoming  $H$ -polarized photon is left untouched, corresponding to the first line in Eq. (1). This process is therefore identical to the decay of a two-level system. Half-wave plate HWPC, oriented at  $0^\circ$ , is used solely to match the lengths of the two optical paths. The path lengths are adjusted so that if HWP1 is oriented at  $0^\circ$ , the polarization state in mode  $a$  after the interferometer is exactly the same as the input state. Photons in modes  $a$  and  $b$  are then directed to the same quantum state tomography (QST) system, composed of a quarter-wave plate QWP2, half-wave plate HWP2, and the polarizing beam splitter PBS2, and then registered using a single-photon detector, equipped with a 10 nm FWHM interference filter, and a 1.5 mm diameter aperture. Mode  $b$  is recombined incoherently with mode  $a$  on PBS2, so that both modes can be detected with a single detector. This is achieved by assuring that the path length difference between modes  $a$  and  $b$  is greater than the coherence length of the photons, which is determined by the width of the interference filters ( $\sim 0.1$  mm). The half-wave plate HWP3, aligned at  $45^\circ$ , transforms  $H$ -polarized photons into  $V$ -polarized ones. Since PBS2 transmits  $H$ -polarization and reflects  $V$ -polarization, the combination of HWP3 and PBS2 reflects photons that were originally  $H$ -polarized. This assures that the QST performed is identical for both modes  $a$  and  $b$ .

Using the interferometer described above, we studied both the decay of a single-qubit and the dynamics of two entangled two-level systems interacting with independent amplitude-decay reservoirs. The experimental setup is shown in Fig. 1b. Polarization-entangled photon pairs with wavelength centered around 884 nm were produced using a standard source [18] composed of two adjacent type-I  $\text{LiIO}_3$  nonlinear crystals pumped by a 441.6 nm c.w. He-Cd laser. One crystal produces photon pairs with  $V$ -polarization and the other produces pairs with  $H$ -polarization. After propagation and spatial mode filtering, the  $H$  and  $V$  modes are spatially indistinguishable, and a photon pair is described by the pure state  $|\Phi\rangle = |\alpha\rangle|HH\rangle + |\beta\rangle e^{i\delta}|VV\rangle$  with high fidelity. A half-

wave plate (HWP) and a quarter-wave plate (QWP), placed in the pump beam, allow the control of the coefficients  $|\alpha|$  and  $|\beta|$ , and the relative phase  $\delta$  of the state [18].

The decay of a single qubit was investigated experimentally for both  $H$  and  $V$ -polarized photons, by generating states  $|VV\rangle$  and  $|HH\rangle$ , and registering coincidence counts, with one photon propagating through the interferometer and the other serving as a trigger. The coincidence detection window ( $c \times 5 \text{ ns} \sim 1.5 \text{ m}$ ) was larger than the path difference between outgoing modes  $a$  and  $b$  ( $\sim 5 \text{ cm}$ ). Fig. 2a shows  $P_V(V)$ ,  $P_H(V)$ ,  $P_V(H)$ ,  $P_H(H)$  as a function of  $p$ , where  $P_J(K)$  is probability of finding an input  $K$ -polarized photon in the  $J$  state after the interferometer. The linear behavior in  $p$  is characteristic of exponential decay in  $t$ , given that  $p = 1 - \exp(-\Gamma t)$ . Vertical error bars were obtained by standard Monte Carlo simulations [20]. The horizontal error bars represent uncertainty in aligning the waveplates.

For the investigation of the entanglement dynamics, non-maximally entangled states were produced, and each photon sent to a separate interferometer, which implemented an amplitude-damping reservoir, and then to a QST system. The half-wave plates HWP1 and HWP4 were set to the same angle  $\theta$ , so that the reservoirs, though independent, acted with the same probability  $p$ . QST of the output two-photon state followed the usual recipe consisting of a set of sixteen coincidence measurements [19]. We repeated the same procedure for different values of  $p$ , obtaining the tomographic reconstruction of the output two-photon polarization state in all cases. The concurrence was calculated using Eqs. (2) and (3).

Figure 2b displays the concurrence, and the quantity  $\Lambda$ , given by Eq. (3), as a function of the decay probability  $p$ , for two initial states that, although not pure, are very close to  $|\Phi\rangle = |\alpha\rangle|HH\rangle + |\beta\rangle e^{i\delta}|VV\rangle$ : state I, defined by  $|\beta|^2 = |\alpha|^2/3$  (triangles), and state II, defined by  $|\beta|^2 = 3|\alpha|^2$  (squares). Tomography of the initial states I and II showed them to have the same concurrence ( $\sim 0.8$ ), and similar purity ( $\sim 0.91 - 0.97$ ). The theoretical curves were obtained by applying map (1) to the experimentally determined initial states, corresponding to  $p = 0$ . As before, the vertical error bars were obtained by Monte Carlo simulation [20]. For initial state I, entanglement disappears asymptotically, and the concurrence goes to zero only when both individual systems have decayed completely ( $p = 1$ ). For initial state II, however, the entanglement behaves very differently: the concurrence goes to zero at a finite time ( $p < 1$ ). This demonstrates ‘‘entanglement sudden death.’’

It is also illustrative to study the purity, defined as  $\text{tr}\rho^2$ , in function of the decay probability, as shown in Fig. 3 for states I and II. We see that in both cases the purity reaches a minimum but is restored when  $p = 1$ , when all photons have ‘‘decayed’’ to the  $H$ -polarization state.

In order to further illustrate the usefulness of the present scheme for studying decoherence of entangled systems, we have performed a second experiment studying the action of a

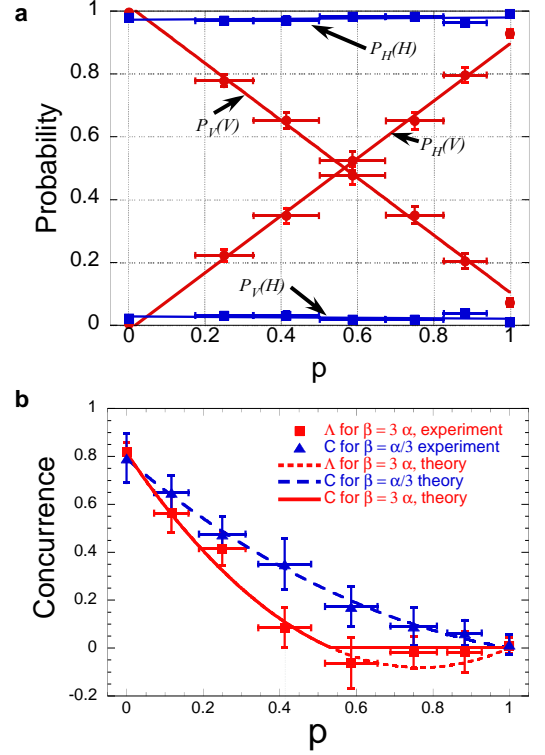


FIG. 2: Results for amplitude decay channel. **a** Experimental amplitude decay for a single qubit.  $P_V(V)$  and  $P_H(V)$  are the probabilities of detecting an input  $V$ -polarized photon in the  $V$  and  $H$  states, respectively.  $P_V(H)$   $P_H(H)$  are the the probabilities for an input  $H$  photon. The points correspond to experimental data, and the lines are linear fits. **b** Entanglement decay as a function of the probability  $p$ . The squares correspond to experimentally obtained values of  $\Lambda$  for the case  $|\beta|^2 = 3|\alpha|^2$ . The solid line is the theoretical prediction of the concurrence for this state, given by Eq. 2, while the dotted line shows the value of  $\Lambda$ , given by Eq. (3). The triangles are experimental values of  $\Lambda$  for the case  $|\beta|^2 = |\alpha|^2/3$ , and the dashed line is the theoretical prediction for  $\Lambda$  and  $C$ , which are equivalent for this state.

pair of dephasing reservoirs, described by the map [1, 2]

$$\begin{aligned} |g\rangle_S \otimes |0\rangle_R &\rightarrow |g\rangle_S \otimes |0\rangle_R \\ |e\rangle_S \otimes |0\rangle_R &\rightarrow \sqrt{1-p}|e\rangle_S \otimes |0\rangle_R + \sqrt{p}|e\rangle_S \otimes |1\rangle_R. \end{aligned} \quad (6)$$

This map represents elastic scattering between atom and reservoir. States  $|e\rangle$  and  $|g\rangle$  are not changed by the interaction, but any coherent superposition of them gets entangled with the reservoir. There is no longer decay, but only loss of coherence between ground and excited states. The dephasing map can be implemented with the same interferometer through the addition of an extra HWP at  $45^\circ$  in mode  $b$  before the QST system (or, equivalently, through the removal of HWP3 and redefinition of the QST measurements). For the dephasing channel, pure states I and II present identical behavior, becoming completely disentangled only when  $p = 1$ . The concurrence (squares) and bipartite purity (triangle) as a function of  $p$  for the entangled state II is shown in Fig. 4. The theoretical pre-

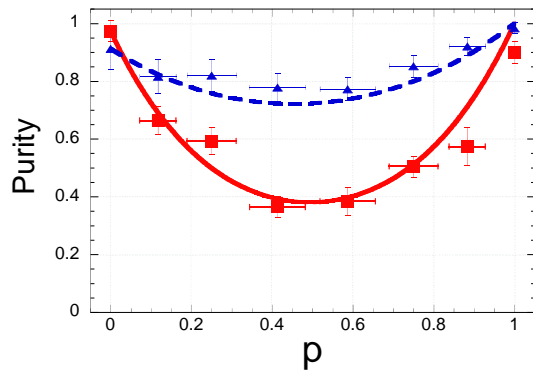


FIG. 3: Purity as a function of  $p$  for the amplitude damping channel. The squares correspond to experimentally obtained values of the purity for the case  $|\beta|^2 = 3|\alpha|^2$ , while the solid line is the theoretical prediction. The triangles are experimental values of the purity for the case  $|\beta|^2 = |\alpha|^2/3$ , and the dashed line is the corresponding theoretical prediction.

diction for the concurrence disappears slightly before  $p = 1$ , due to the fact that the initial state is not 100% pure.

In conclusion, we have reported an experimental demonstration of the sudden disappearance of the entanglement of a bipartite system, induced by the interaction with an environment. We have shown that entangled states with the same initial concurrence may exhibit, for the same reservoir, either an abrupt or an asymptotic disappearance of entanglement, in spite of the fact that the constituents of the system always exhibit an asymptotic decay. We have explicitly demonstrated that this behavior also depends on the characteristics of the reservoir, through two examples, corresponding to amplitude

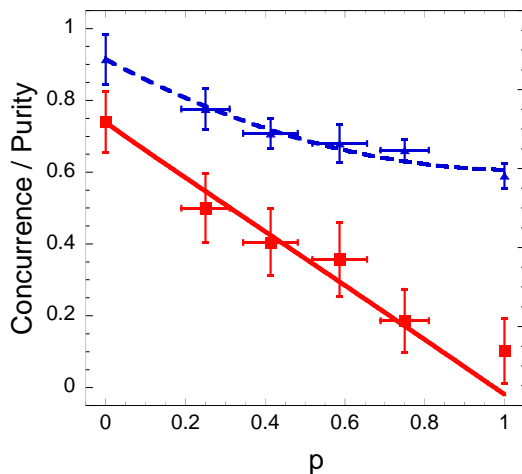


FIG. 4: Experimental results for the dephasing reservoir. Concurrence (squares) and purity (triangles) are shown for the case  $|\beta|^2 = 3|\alpha|^2$ . The solid line is the corresponding theoretical prediction for concurrence, given by Eq. (2). The dashed line is the theoretical prediction for purity, given by  $\text{tr}\rho^2$ . The concurrence goes to zero asymptotically.

decay and dephasing. The experimental setup represents a reliable and simple method for studying decoherence of entangled systems interacting with controlled reservoirs.

The authors acknowledge financial support from the Brazilian funding agencies CNPq, CAPES, PRONEX, FUJB and FAPERJ. This work was performed as part of the Brazilian Millennium Institute for Quantum Information.

\* swalborn@if.ufrj.br

- [1] Nielsen, M. A. & Chuang I, *Quantum Computation and Quantum Information* (Cambridge University Press, Cambridge, U.K., 2000).
- [2] Preskill, J. *Lecture notes on quantum information and computation*. Available at <http://www.theory.caltech.edu/people/preskill/ph219/>.
- [3] Bennett, C. H. & DiVincenzo, D. P. Quantum information and computation. *Nature* **404**, 247-255 (2000).
- [4] Bennett, C. H. & Brassard, G. in *Proc. IEEE Int. Conf. on Computers, Systems and Signal Processing* 175-179 (IEEE, New York, 1984).
- [5] Ekert, A. Quantum cryptography based on Bell's theorem. *Phys. Rev. Lett.* **67**, 661-663 (1991).
- [6] Gisin, N. *et al.*, Quantum Cryptography, *Rev. Mod. Phys.* **74** 145 (2002).
- [7] Bennett, C. H. *et al.* Teleporting an unknown quantum state via dual classical and Einstein-Podolsky-Rosen channels. *Phys. Rev. Lett.* **70**, 1895-1898 (1993).
- [8] Bouwmeester, D. *et al.* Experimental quantum teleportation. *Nature* **390**, 575-579 (1997).
- [9] Boschi D. *et al.* Experimental Realization of Teleporting an Unknown Pure Quantum State via Dual Classical and Einstein-Podolsky-Rosen Channels. *Phys. Rev. Lett* **80**, 1121 (1998).
- [10] Duan, L.-M., Lukin, M. D., Cirac, J. I., & Zoller, P. Long-distance quantum communication with atomic ensembles and linear optics. *Nature* **414**, 413-418 (2001).
- [11] Zurek, W. H. Decoherence, einselection, and the quantum origins of the classical. *Rev. Mod. Phys.* **75**, 715-775 (2003).
- [12] Diósi, L. in *Irreversible Quantum Dynamics*, edited by F. Benatti and R. Floreanini (Springer, Berlin, 2003).
- [13] P. J. Dodd, P. J. & Halliwell, J. J. Disentanglement and decoherence by open system dynamics. *Phys. Rev. A* **69**, 052105 (2004).
- [14] Yu, T. & Eberly, J. H. Finite-time disentanglement via spontaneous emission. *Phys. Rev. Lett.* **93**, 140404 (2004).
- [15] Santos, M. F., Milman, P., Davidovich, L. & Zagury, N., Direct measurement of finite-time disentanglement induced by a reservoir, *Phys. Rev. A* **73**, 040305(R) (2006).
- [16] Yu, T & Eberly, J. H. Quantum open system theory: Bipartite aspects. *Phys. Rev. Lett.* **97**, 140403 (2006).
- [17] Wootters, W. K. Entanglement of formation of an arbitrary state of two qubits. *Phys. Rev. Lett.* **80**, 2245-2248 (1998).
- [18] Kwiat, P. G. *et al.*, Ultrabright source of polarization-entangled photons, *Phys. Rev. A* **60** R773 (1999).
- [19] James D. V. *et al.*, Measurement of qubits, *Phys. Rev. A* **64** 052312 (2001).
- [20] Altepeter, J. B. *et al.*, Photonic State Tomography, *Advances in Atomic, Molecular and Optical Physics*, Elsevier (2005).